EFDA–JET–PR(07)28

A. Eriksson, H. Nordman, P. Strand, J. Weiland, T. Tala, E. Asp, G. Corrigan, C. Giroud, M de Greef, I. Jenkins, H.C.M. Knoops, P. Mantica, K.M. Rantamäki, P.C. de Vries, K.-D. Zastrow and JET EFDA contributors

Predictive Simulations of Toroidal Momentum Transport at JET

Predictive Simulations of Toroidal Momentum Transport at JET

A. Eriksson[1], H. Nordman[1], P. Strand[1], J. Weiland[1], T. Tala[2], E. Asp[3], G. Corrigan[4], C. Giroud[4], M de Greef[5], I. Jenkins[4], H.C.M. Knoops[5], P. Mantica[6], K.M. Rantamäki[2], P.C. de Vries[4], K.-D. Zastrow and JET EFDA contributors*

JET-EFDA, Culham Science Centre, OX14 3DB, Abingdon, UK

[1] Chalmers University of Technology, EURATOM/VR Association, Göteborg, Sweden
[2] VTT Technical Research Centre of Finland, EURATOM-Tekes, Espoo, Finland
[3] EPFL-CRPP, Association Euratom-Confédération Suisse, CH-1015 Lausanne, Switzerland
[4] EURATOM/UKAEA Fusion Association, Culham Science Centre, Abingdon, OX14 3DB, UK
[5] Department of Applied Physics, Eindhoven University of Technology, Eindhoven, The Netherlands
[6] Istituto di fisica del plasma, Associazione Euratom-ENEA-CNR, Milan, Italy
** See annex of M.L. Watkins et al, "Overview of JET Results ", (Proc. 21st IAEA Fusion Energy Conference, Chengdu, China (2006)).*

Preprint of Paper to be submitted for publication in
Physical Review Letters

ABSTRACT

A new version of the Weiland model has been used in predictive JETTO simulations of toroidal rotation. The model includes a self-consistent calculation of the toroidal momentum diffusivity (χ_ϕ) which contains both diagonal and non-diagonal (pinch) contributions to the momentum flux. Predictive transport simulations of JET H-mode, L-mode and hybrid discharges are presented.

It is shown that experimental temperatures and toroidal velocity were well reproduced by the simulations. The model predicts the ion heat diffusivity (χ_i) to be larger than the momentum diffusivity and it gives Prandtl numbers ($Pr = \chi_\phi/\chi_i$) between 0.1 and 1. The Prandtl numbers are often, depending on the plasma conditions, predicted to be significantly smaller than unity. This is in accordance with experimental findings.

1. INTRODUCTION

Toroidal momentum transport in fusion devices needs to be well understood since rotation of the plasma may suppress turbulence and thus affect the performance of the device. This is of particular importance for the prediction of ITER scenarios where low levels of toroidal rotation are expected due to the large inertia and low torque compared to present devices. It is also important to understand the toroidal momentum transport in plasmas with Internal Transport Barriers (ITB) in present devices since momentum transport generates rotational shear which is important for the formation of ITBs [1].

Previously, it has generally been assumed that both the global confinement times and the diffusivities of energy and momentum are equal under steady state conditions [2, 3, 4]. More recent experimental studies do however contradict the general validity of this theory [5]. It has also recently been shown for JET discharges that similar confinement times may very well be combined with momentum diffusivities (χ_ϕ) that are significantly smaller than the ion heat diffusivities (χ_i) in the core of the plasma [6]. Experimental Prandtl numbers ($Pr = \chi_\phi/\chi_i$) were found to be about 0.3 for high density H-mode discharges and they were also found to be dependent on the plasma parameters.

In predictive simulations of tokamak discharges, toroidal velocity has usually been treated interpretatively. Attempts to model the toroidal velocity with the assumption that the toroidal momentum diffusivity is equal to the ion heat diffusivity fail and give too small rotation compared to experiment. With the assumption that $Pr \approx 1/3$ the predicted toroidal rotation gets closer to the experimental values. There seems, however, not to be any clear scaling of the Prandtl number. This is why we need to calculate the momentum diffusivity self-consistently.

In the present paper we present new predictive simulations of high density type I ELMy H-mode, low density H-mode, L-mode and hybrid JET discharges. The simulations are based on Ion Temperature Gradient (ITG) and Trapped Electron (TE) mode driven transport of heat and toroidal momentum [7, 8]. The temperature and toroidal velocity profiles are compared with experiments using the JETTO transport code [9]. The Prandtl numbers are calculated in steady state and the role of the momentum pinch is examined.

The paper is organised as follows. In Section 2 a brief summary of the transport model we use is given. Section 3 contains parameter scalings of the Prandtl number. In Section 4 the method used for our simulations is presented. Section 5 contains information about the discharges we have simulated.

In Section 6 our results are presented. The discussions are found in Section 7 and the last section contains our conclusions.

2. TOROIDAL MOMENTUM TRANSPORT MODEL

The transport model we use here has been described in detail elsewhere [7, 8]. A brief summary with focus on the toroidal momentum transport is given here. The model describes quasilinear transport due to ITG and TE mode turbulence using fluid descriptions for the ion and trapped electron species. The particle, heat and toroidal momentum fluxes (Γ_n, Γ_T, Γ_ϕ) and their corresponding effective diffusivities (D, χ, χ_ϕ) are obtained from the time average of the ITG/TE mode perturbations in density (n), temperature (T), and toroidal velocity (v_ϕ) as $\Gamma_n = Re < v^*_{Er}\delta n > = -D\nabla n$, $\Gamma_T = Re < v^*_{Er}\delta T > = \chi\nabla T$ and $\Gamma_\phi = m_i n\, Re < v^*_{Er}\delta v_\phi > = m_i n\chi_\phi \nabla v_\phi$ where v_{Er} is the E×B drift velocity, " means complex conjugate and mi is the mass of the main ions.

The relation $v_\phi \approx v_{||} - (B_\theta/B)v_\theta$ between the toroidal and parallel velocity is used to calculate the toroidal momentum flux. The parallel ion velocity perturbation ($\delta v_{||i}$) is calculated from the parallel momentum balance in the presence of a zero order background flow as

$$\delta v_{||i} = \frac{k_\theta \rho_s c_s}{\omega}\frac{dv_{||}}{dr}\,\hat{\phi} + \frac{k_{||}c_s^2}{\omega}\left(\hat{\phi} + \frac{1}{\tau}P - \frac{\tilde{\omega} + (1+\eta_i/(\in_n\tau)}{k_{||}\tilde{c}_s}\,\hat{\mathrm{A}}_{||}\right) \tag{1}$$

where the first term is the E×B convection of the background velocity.

In our notation $\omega = \omega_r + i\gamma$ is the wave frequency, $\eta_i = L_n/L_{Ti}$ is the ratio of density to temperature length scales, $\in_n = 2L_n/R$, $\tau = T_e/T_i$ is the temperature ratio, ρ_s is the gyroradius, c_s is the ion acoustic velocity, k_θ, $k_{||}$ and k_x are the wave numbers in the poloidal, parallel and radial directions, respectively. Further, ~ denotes normalisation by …De which is the electron drift frequency due to the magnetic gradient and curvature, $\omega_{Dj}(j = e, i) = \boldsymbol{k}\cdot\boldsymbol{v}_{Dj}$ where $\boldsymbol{v}_{Dj} = T_j/(m_j\Omega_j)\hat{\boldsymbol{b}}\times(\nabla B/B + \hat{b}\cdot\nabla\hat{b})$, with Ω_j as the gyrofrequency and $\mathbf{B} = B\hat{\mathbf{b}}$. We also use $\hat{\phi} = e\phi/T_e$ and $\hat{A}_{||} = eA_{||}/T_e$ which are the normalised electrostatic and electromagnetic potentials, respectively. The normalised pressure perturbation, which is also a function of $\hat{\phi}$, is denoted $\hat{P} = \delta P/P_0$.

Neglecting poloidal flow terms, the diagonal toroidal momentum flux is derived from quasi-linear theory with $v_{Ex} = -ik_\theta/B$ and $\delta v_\phi = -k_\theta\rho_s c_s/\omega d_\phi/dr\,\hat{\phi}$. Assuming that E×B convection is the main non-linear saturation mechanism the potential fluctuation is given by $\hat{\phi} = \gamma/(k_x\rho_s k_\theta c_s)$ [10]. The second term in equation (1) gives off-diagonal pinch terms proportional to $< k_{||} >$ and the total toroidal momentum flux is thus approximated as [8]

$$\Gamma_\phi \approx -m_i n\,\frac{\gamma^3/k_x^2}{\omega_r^2/\gamma^2}\,\frac{dv_\phi}{dr} + <k_{||}> f(\hat{\phi}, \hat{P}, \hat{A}_{||}) \tag{2}$$

Here, we will assume that the poloidal velocity is well described by neoclassical theory.

In Equation (2), the first term is the diagonal diffusion and the second term represents the off-diagonal pinch terms proportional to $< k_{||} >$. The diagonal term is usually the dominant term for toroidal momentum transport in the present model. The off-diagonal pinch terms are proportional to the flux surface average of $k_{||}$ which is zero for standard drift waves with up-down symmetric eigenfunctions. Radial flow shear (dv_ϕ/dr, dv_θ/dr) can produce a mode shift which leads to a finite value of $< k_{||}>$ and this may lead to an inward flow of toroidal momentum [11, 11, 12]. We use a previously derived eigenfunction to calculate $<k_{||}>$ [13].

A significant toroidal momentum pinch due to Coriolis drift effects, not included in the present study, has recently been reported [14]. This pinch is however associated with larger diagonal momentum terms as well and the net effect is still under investigation.

3. PARAMETER SCALINGS

In order to obtain a simple estimate of the scaling and magnitude of the Prandtl number $Pr = \chi_\phi/\chi_i$, we will in this section neglect the pinch contributions to the toroidal momentum flux. The effect of the momentum pinch will be discussed in Section 7. We focus here on parameter scalings that are of relevance for the analysis of the simulated JET discharges, namely scalings with R/L_T and R/L_n since different peaking factors are expected for the considered low and high density discharges. In addition, we investigate the sensitivity of the Prandtl number to the driving instability (ITG vs TE mode).

First, we consider some basic properties of the derived Prandtl number. The main diagonal momentum diffusivity can be written as

$$\chi_\phi = \frac{\gamma^3/k_x^2}{\omega_r^2/\gamma^2} \tag{3}$$

The ion heat diffusivity is calculated using the ion temperature perturbation given by energy balance as

$$\delta T_i = \frac{\omega \mathrm{T}_i}{\omega - 5\omega_{Di}/3}\left(\frac{2}{3}\,\hat{n}_i + \frac{\eta_i - 2/3}{\in_n \tilde{\omega}}\,\hat{\phi}\right) \tag{4}$$

where $\hat{n}_i = \delta n_i/n_0$ is the density perturbation. This gives a diagonal ion heat diffusivity ($\chi_i = (\gamma^3/k_x^2)/((\omega_r - 5/3\omega_{Di})^2 + \gamma^2)$) with a resonance due to the toroidal effects that enters through ω_{Di} (non-Markovian mixing length). This mixing length is a fundamental reason why the model gives a Prandtl number deviating from unity. The Prandtl number is approximated as

$$P_r \approx \frac{(\omega_r - 5/3\omega_{Di})^2 + \gamma^2}{\omega_r^2/\gamma^2} \tag{5}$$

This simple expression shows that for strong turbulence ($\gamma >> \omega_r$) the Prandtl number approaches

unity, in accordance with some early predictions of momentum transport from ITG theory [2]. We also note that for modes rotating in the ion drift direction, $Pr < 1$ is obtained whereas for modes rotating in the electron drift direction we obtain $Pr > 1$. In the following, the scaling of Pr will be illustrated by neglecting the usually small contributions from the momentum pinch but including the complete expression for the ion heat flux [2, 7].

In Figure 1 the Prandtl number $Pr = \chi_\phi/\chi_i$ versus the normalised temperature scale length $R/L_{Ti} = R/L_{Te}$ is displayed for an ITG mode dominated case neglecting trapped electrons (i.e. trapped particle fraction $f_t = 0$, solid) and for a trapped particle fraction $f_t = 0.5$ (dotted), with $R/L_n = 3$, $\tau = 1$, safety factor $q = 1.4$, and magnetic shear $s = 1$. The normalised wave frequencies are also shown in Figure 1; the negative real frequency (dotted) together with the larger growth rate (solid) correspond to the dominant ITG mode, whereas the positive real frequency and the smaller growth rate (dashdotted) correspond to the present but weaker TE mode. As observed, the Prandtl number increases with R/L_T as the dominating ITG mode is further destabilised, in accordance with the qualitative discussion above. The Prandtl number also increases as the TE mode is introduced for $f_t = 0.5$. The upshift of the curve for $f_t = 0.5$ is mainly a result of a decrease in the heat flux driven by TE mode turbulence.

Figure 2 displays the scaling of the Prandtl number with the normalised density scale length R/L_T. The wave frequencies are also shown. The scaling with R/L_n is weaker than that obtained for the temperature scale length, butthe trend is similar: a more peaked profile results in a larger Prandtl number. As already observed in Figure 1, the onset of the TE mode ($f_t = 0.5$) leads to a larger Prandtl number.

The result of these theoretical investigation is that the ratio χ_ϕ/χ_i can vary significantly depending on the plasma conditions, from relatively small values ($Pr << 1$) for flat profiles that are ITG dominated to ratios around unity for peaked profiles or plasmas with significant contributions to transport from TE mode turbulence or strong turbulence in general. The non-diagonal contributions to the momentum transport may change the details of these conclusions, but the main trends should be unaffected. We expect that the neglected momentum pinch would tend to reduce the Prandtl numbers further by reducing the effective momentum diffusivity.

4. SIMULATIONS

In order to compare our theoretical understanding of the scaling of the Prandtl number with experimental findings predictive JETTO [9] simulations of temperature (T_e, T_i) and toroidal velocity (v_ϕ) profiles have been made using the new version of the Weiland model described in Section 2. Previous versions of the model, neglecting toroidal momentum transport, have been successful in describing core heat transport in JET L- mode and H-mode plasmas [15, 16].

In the simulations both diagonal (diffusive) and non-diagonal (pinch) contributions to the toroidal momentum transport have been included. For some discharges only the diagonal contribution has been kept due to issues of numerical instability.

Starting from the experimental steady state profiles as initial conditions, the simulations follow

the temperatures and toroidal velocity until a stationary state is reached, typically within 0.5 – 1 seconds, which is several times the energy confinement time of typical JET plasmas. The main ion and impurity density profiles are kept fixed at their experimental values.

The boundary condition at the normalised radius $r/a = 0.8$ for temperatures and toroidal velocity are matched as closely as possible in the simulations by adjusting the JETTO boundary condition at $r/a = 1$.

5. ANALYSED DISCHARGES

The discharges simulated in this study are six high density type I ELMy H-mode and six low density (H-mode, L-mode and hybrid) JET discharges, see Table 1 for experimental data. The ion temperature and toroidal velocity profiles were obtained using Charge Exchange Recombination Spectroscopy (CXRS), assuming that main ions and carbon ions have equal temperature and velocities. The discharges are heated by Neutral Beam Injection (NBI) combined with a small fraction of on-axis Ion Cyclotron Resonant Heating (ICRH). NBI is the dominant source of toroidal momentum for the considered discharges. The NBI heat and torque deposition used in the simulations are computed using the PENCIL code [17], see Figure 3 for examples of calculated profiles.

The momentum and heat transport in the high density H-mode discharges have been analysed in a previous experimental study [6]. The discharges are characterised by relatively flat profiles of density ($R/L_n < 2$) and toroidal velocity, and approximately equal ion and electron temperatures. The torque deposition profile is hollow at high densities, Figure 3. The high collisionality in these plasmas tends to stabilise the TE mode leaving the ITG mode as the dominant instability. Three of the H-mode discharges, the L-mode and the hybrid discharges have low density and peaked torque deposition profiles, Figure 3. The temperature scale length R/L_T varies between 3 and 9 in the analysed discharges.

The Prandtl numbers calculated from experimental measurements were found to be significantly below unity, with $0.18 < Pr < 0.35$ for the high density discharges and $0.24 < Pr < 0.51$ for the low density discharges. This is in conflict with the assumption typically used for ITER predictions of $Pr = 1$. However, the low Prandtl numbers are in agreement with the theoretical estimates of Section 3 where $Pr << 1$ were obtained for ITG dominated discharges, in particular for flat temperature profiles.

6. RESULTS

The main results of the simulations are summarised in Table 2, which gives the relative errors (δ), Root-Mean-Square (RMS) errors (σ), and Prandtl numbers. The results are averaged over the resulting profiles (T_i, T_e, v_ϕ, χ_ϕ/χ_i) at $0.4 < r/a < 0.7$. The errors are defined as $\delta = 1/N \, \Sigma_{i=1}^{N} (f_i^{sim} - f_i^{exp})/f_i^{exp}$ *and* $\sigma = (1/N \, \Sigma_{i=1}^{N} ((f_i^{sim} - f_i^{exp})/f_i^{exp})^2)^{1/2}$. Table 1 also shows in what simulations the pinch terms are included and what modes that are clearly unstable.

The average RMS errors for the simulated high density discharges are $\sigma_{Te} = 13\%$, $\sigma_{Ti} = 11\%$ and $\sigma_{v\phi} = 14\%$ respectively. The resulting Prandtl numbers are well below unity, with $0.13 < Pr < 0.35$.

This is to compare with the experimental Prandtl numbers for these discharges, i.e. $0.18 < Pr < 0.35$.

For the low density discharges the average RMS errors are $\sigma_{Te} = 9\%$, $\sigma_{Ti} = 9\%$ and $\sigma_{v\phi} = 22\%$. The resulting Prandtl numbers are $0.39 \lesssim Pr$ 1, which we compare with the experimental values $0.24 < Pr < 0.51$.

The linear eigenvalues have been studied with the fluid model used here and with the linear gyrokinetic code Kinezero [18]. The result of this analysis is that all discharges studied here, except Pulse No: 59217, are ITG dominated. The high density discharges in this study are clearly ITG dominated. The low density discharges have unstable ITG and TE modes with growth rates of about the same size.

Figures 4 and 5 display the predicted and experimental temperature and toroidal velocity profiles versus radius for Pulse No's: 57865 and 57871, respectively. The Prandtl numbers versus normalised radius are also shown. In these simulations, both the main diagonal term in the effective momentum diffusivity and the momentum pinch terms were included. Both temperature and velocity profiles are overpredicted ($\delta > 0$), which is typical for most of the simulated high density discharges. The Prandtl numbers are subject to numerical instabilities due to the pinch in the edge and inner core region.

Figures 6 and 7 show predictions for the low density L-mode and hybrid Pulse No's: 55809 and 60931, respectively. Both temperatures and toroidal velocity are underpredicted ($\delta < 0$). In these simulations the momentum pinch terms are not included due to large numerical instabilities. The Prandtl numbers are also displayed in the Figures, which show that they increase with radius.

A simulation of the low density H-mode Pulse No: 59217 is displayed in Figure 8. Here the temperatures are overpredicted and the toroidal velocity underpredicted. The pinch terms are not included due to issues of numerical instability. Also in simulations of the low density H-mode Pulse No: 59218 where the momentum pinch terms are included the temperatures are overpredicted and the toroidal velocity underpredicted. The Prandtl number is also shown and it increases with radius and becomes larger than unity in some regions, which is also the case for the low density H-mode Pulse No's: 59218 and the L-mode 55809.

Figure 9 displays a comparison of the predicted momentum profile and Prandtl numbers for Pulse No: 57894 with and without the momentum pinch included in the simulations. This is the discharge for which the pinch terms have the most significant impact on the result of the simulations. The pinch terms increase the toroidal velocity and decrease the Prandtl number ($Pr = 0.24$ versus $Pr = 0.16$ respectively). There are numerical instabilities in the edge and inner core region when the pinch is included in the simulation.

DISCUSSION

In general the agreement between the predicted and experimental profiles is good outside the inner core region ($r/a > 0.3$) where the profiles tend to be overpredicted due to stabilization of the ITG

mode. The model reproduce temperature profiles well in both high and low density discharges. The toroidal velocity profiles were also well reproduced in the high density discharges (small overprediction) and the agreement is slightly worse in the low density discharges (underprediction). This is reflected in the result for the Prandtl numbers where we find better agreement between simulation and experiment for the high density discharges.

A main feature of the simulations presented here is that they give Prandtl numbers in approximate agreement with experiment. They differ significantly from predictions of early slab ITG theory as discussed in Section 3 and are in most of the simulations below unity. The lower Prandtl numbers are, in the present model, possible due to the toroidal effects and the non-Markovian mixing length. Toroidal effects alone may be included in ITG models and still give $Pr = 1$ if a more simple mixing length rule is used.

There is a span of about one order of magnitude in the simulated Prandtl numbers. There are different possible explanations hereto, of which some are physical and and some are model artefacts. The experimentally derived Prandtl numbers do not show such a wide span.

First, one important factor is which mode that is dominant in the discharge. TE mode dominated discharges are expected to have larger Prandtl numbers than pure ITG mode shots, as shown in Section 3. This effect is seen in both experiments and simulations where the clearly ITG dominated high density discharges in this study have smaller Prandtl numbers than the low density discharges that all have strongly excited TE modes.

Secondly, the Prandtl number is affected by the slope of the temperature and density profiles. A flatter density profile is usually associated with a weaker non-diagonal heat flux, and thus leads to a lower Prandtl number. Among the discharges simulated here the high density H-modes and the hybrid have flat density profiles. This might thus be the reason for the lower Prandtl number in the hybrid discharge compared to the other low density dischares.

A third factor is that strong turbulence is prediced to increase the Prandtl number. In L-mode the transport is higher, probably due due to stronger turbulence. The L-mode discharges simulated here accordingly have the largest Prandtl numbers.

The magnitudes of these effects might however differ between simulations and experiment. We clearly see the same trend that the low density discharges have larger Prandtl numbers combined with stronger TE modes, less flat profiles and stronger turbulence than the high density discharges. The uncertainties in the simulated toroidal velocites are though too large in some of the simulations for more exact determination of the Prandtl numbers in each case.

The momentum pinch terms as they are defined here seem to have a small effect on the Prandtl number. They do, however, usually reduce the effective momentum diffusivity in the simulations, resulting in a lower Prandtl number and a somewhat larger rotation velocity, Figure 9. We have verified that the effect of the momentum pinch on the velocity profiles is even smaller for the other simulated high density discharges. The pinch may be important in the low density discharges due to the larger velocity shear caused by the more peaked torque profiles, but numerical problems make

them difficult to simulate. Small velocity shear gives small $< k_{||} >$ and thus small pinch terms. The missing pinch term is a probable cause to the worse agreement between simulation and experiment in the low density discharges compared to the high denisty discharges.

CONCLUSIONS

We have theoretically verified that the Prandtl number deviates from the previous assumption of unity. For ITG mode dominated discharges it is up to one order of magnitude smaller than unity. Strong TE modes, peaked profiles and strong turbulence increase the Prandtl number.

The version of theWeiland model used here is able to reproduce experimental Prandtl numbers. The main contribution to the toroidal momentum diffusivity is the outward diagonal diffusion. Off-diagonal pinch terms slightly reduce the Prandtl number.

Having low Prandtl numbers in flat density H-mode discharges is promising for ITER scenarios with flat density profiles. Low Prandtl numbers may imply that a small central torque is sufficient to maintain a peaked momentum profile, which would give a stabilising shear flow.

REFERENCES

[1]. Parail VV 2002 Plasma Physics and Controlled Fusion **44** A63

[2]. Mattor N. and Diamond PH 1988 Physics of Fluids **31** 1180

[3]. Zastrow K-D et al 1998 Nuclear Fusion **38** 257

[4]. deGrassie J.S. et al 2003 Nuclear Fusion **43** 142

[5]. Nishijima D. et al 2005 Plasma Physics and Controlled Fusion **47** 89

[6]. de Vries P.C. et al 2006 Plasma Physics and Controlled Fusion **48** 1693

[7]. Weiland J. 2000 Collective modes in inhomogeneous plasma (Plasma physics series) Bristol:Institute of physics publishing

[8]. Weiland J. and Nordman H. 2006 33rd EPS Conference on Plasma Physics **301** 2.186 (Rome: ECA)

[9]. Cenacchi G. and Taroni A. 1988 Jetto: A free-boundary plasma transport code (basic version) Technical report

[10]. Nordman H. and Weiland J. Nuclear Fusion **29** 251

[11]. Dominguez R.R. and Staebler G.M. Physics of Fluids B **5** 3876

[11]. Garbet X., Sarazin Y. and Ghendrih P. 2002 Physics of Plasmas **9** 3893

[12]. Peeters A.G. and Angioni C. 2005 Physics of Plasmas **12** 072515

[13]. Davydova T.A. and Weiland J. 2000 Physics of Plasmas **7** 243

[14]. Peeters A.G., Angioni C and Strintzi D 2007 Physical Review Letters **98** 265003

[15]. Frojdh M. et al 1996 Plasma Physics and Controlled Fusion **38** 325

[16]. Strand P. et al 1998 Nuclear Fusion **38** 545

[17]. Challis C.D. et al 1989 Nuclear Fusion **29** 563

[18]. Bourdelle C. et al 2002 Nuclear Fusion **42** 892

Type	No	B_{tor} (T)	I_p (MA)	P_{NBI} (MW)	$n_e(0)$ 10^{19} m^3)	$T_e(0)$ (keV)	$T_i(0)$ (keV)	T_e/T_i	$v_\phi(0)$ (km=s)
High	57865	2.7	2.5	13.5	10.0	3.6	3.7	1.0	150
density	57871	2.7	2.5	13.5	8.1	4.1	5.0	0.8	156
H-mode	57886	2.7	2.5	15.0	10.5	3.5	4.5	0.8	204
	57889	2.7	2.5	13.5	11.5	4.6	3.9	1.2	152
	57894	2.7	2.5	13.4	8.6	3.8	4.7	0.8	116
	57896	2.7	2.5	13.4	7.2	5.2	5.9	0.9	166
Low	59215	2.9	1.9	10.0	4.2	5.4	8.0	0.7	240
density	59217	2.9	1.9	11.6	5.2	5.0	6.6	0.8	216
H-mode	59218	2.9	1.9	9.8	4.7	4.2	5.2	0.8	189
L-mode	55807	3.25	1.6	6.0	3.4	3.8	4.1	0.9	105
	55809	3.25	1.6	9.1	3.4	5.0	4.7	1.1	120
Hybrid	60931	1.7	1.4	16.8	3.6	3.8	4.1	0.9	118

Table 1: Experimental data for the JET discharges analysed in this study

Type	No	δ_{T_e} (%)	σ_{T_e} (%)	δ_{T_i} (%)	σ_{T_i} (%)	$\delta_{v\phi}$	$\sigma_{v\phi}$ (%)	Pr (%)	Pinch in sim	Mode
High	57865	12	13	11	12	8	9	0.35	yes	ITG
density	57871	5	7	1	4	-3	5	0.22	yes	ITG
H-mode	57886	31	31	25	26	28	29	0.21	yes	ITG
	57889	-2	3	9	10	8	9	0.13	yes	ITG
	57894	16	16	13	13	3	9	0.16	yes	ITG
	57896	6	7	2	3	23	23	0.20	yes	ITG
Low	59215	23	27	11	17	-14	14	0.69	no	ITG/TE
density	59217	3	4	2	2	-14	14	0.72	no	ITG/TE
H-mode	59218	1	2	1	2	-41	41	1	yes	ITG/TE
L-mode	55807	0	3	5	7	-30	31	0.88	no	ITG/TE
	55809	-7	7	-6	11	-16	18	1	no	ITG/TE
Hybrid	60931	-12	12	-16	16	-14	15	0.39	no	ITG/TE

Table 2: Relative errors (δ), RMS errors (σ) and Prandtl numbers for the simulated JET discharges; the last two columns show if the pinch terms are included or not and what modes that are unstable, respectively, in the simulations. All values are averaged over the radius at $0.4 < r/a < 0.7$

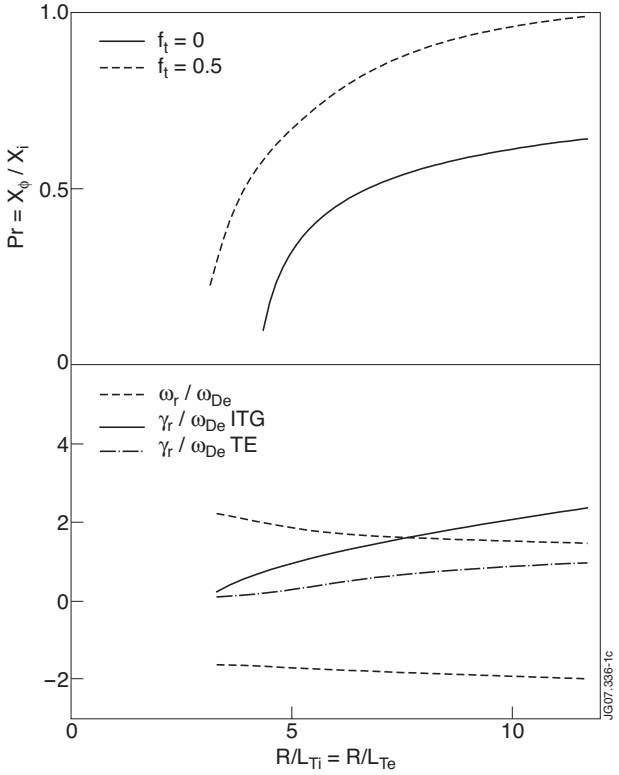

Figure 1: Prandtl number $Pr = \chi_\phi/\chi_i$ versus $R/L_{Ti} = R/L_{Te}$ for trapped particle fractions $f_t = 0$ and $f_t = 0.5$, respectively (above); other parameters are $R/L_n = 3$, $\tau = 1$, magnetic shear $s = 1$, and safety factor $q = 1.4$. Real frequencies (ω_r) and growth rates (γ) are shown for the case with ft = 0.5 (below).

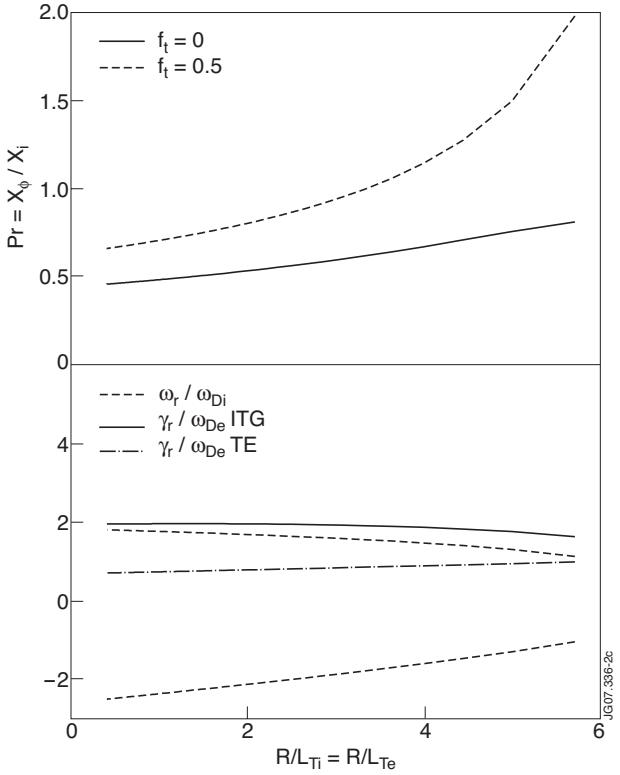

Figure 2: Prandtl number $Pr = \chi_\phi/\chi_i$ versus R/L_n for trapped particle fractions $f_t = 0$ and $f_t = 0.5$, respectively (above); other parameters are $R/L_{Ti} = R/L_{Te} = 9$, $\tau = 1$, magnetic shear $s = 1$, and safety factor $q = 1.4$. Real frequencies (ω_r) and growth rates (γ) are shown for the case with $f_t = 0.5$ (below).

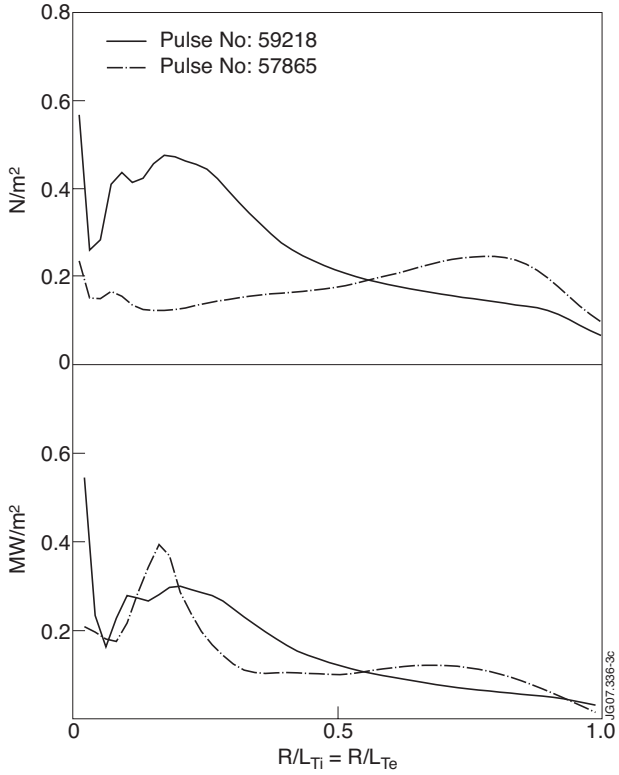

Figure 3: Torque (above) and power deposition (below) profiles for the low density JET Pulse No: 59218 (solid) and for the high density JET Pulse No: 57865 (dash-dotted).

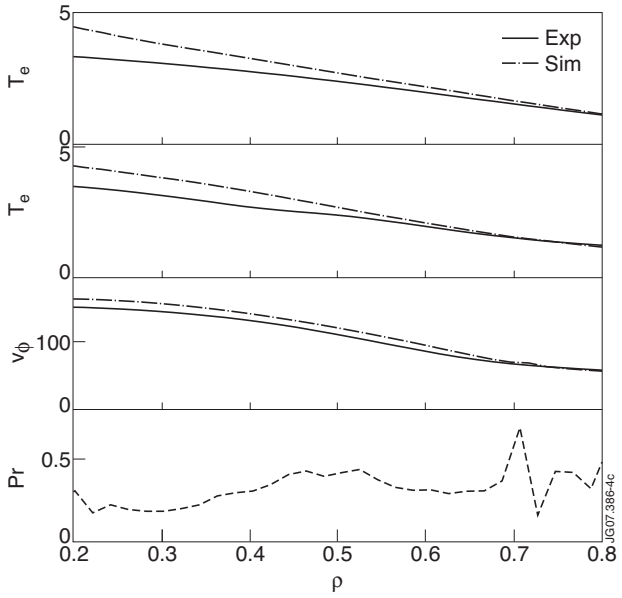

Figure 4: Experimental and predicted temperature and toroidal velocity profiles for JET Pulse No: 57865; predicted Prandtl numbers are also shown.

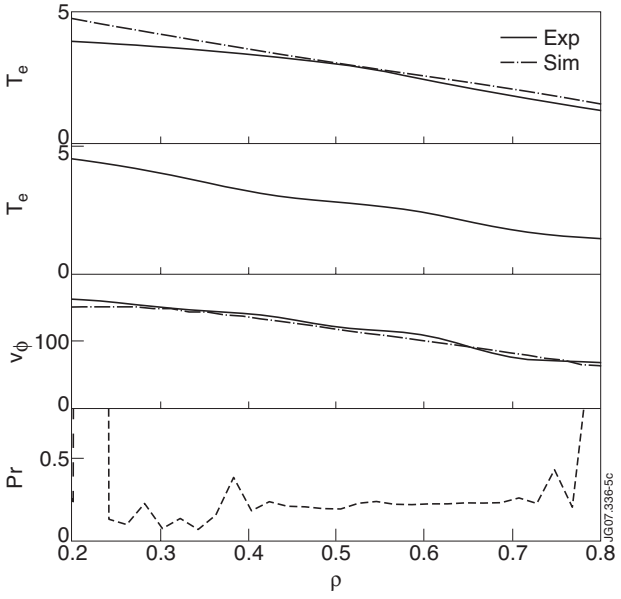

Figure 5: Experimental and predicted temperature and toroidal velocity profiles for JET Pulse No: 57871; predicted Prandtl numbers are also shown.

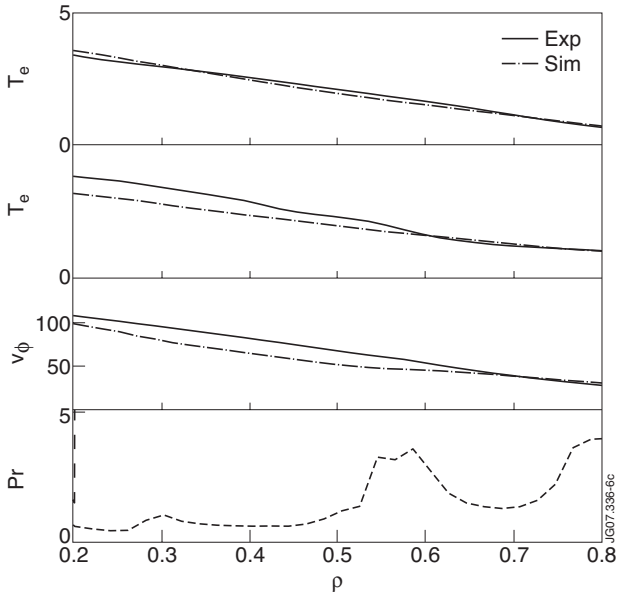

Figure 6: Experimental and predicted temperature and toroidal velocity profiles for JET Pulse No: 55809; predicted Prandtl numbers are also shown.

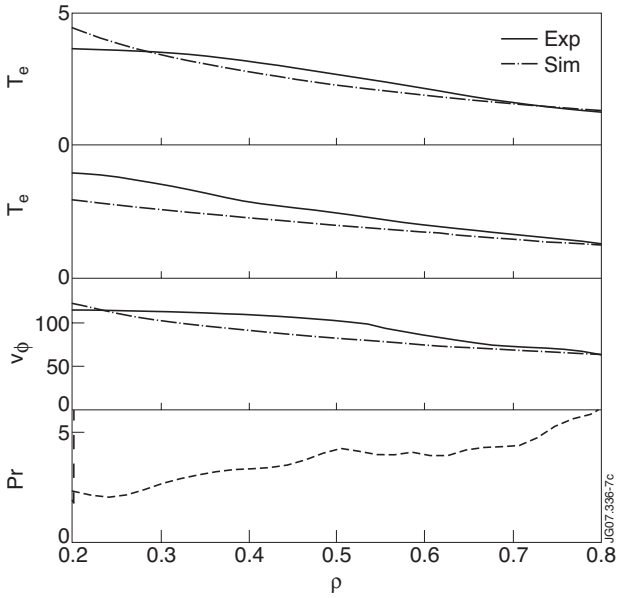

Figure 7: Experimental and predicted temperature and toroidal velocity profiles for JET Pulse No: 60931; predicted Prandtl numbers are also shown.

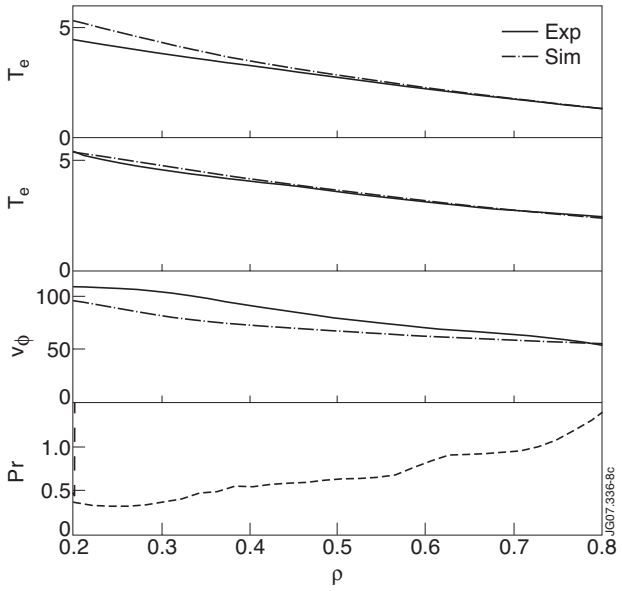

Figure 8: Experimental and predicted temperature and toroidal velocity profiles for JET Pulse No: 59217; predicted Prandtl numbers are also shown.

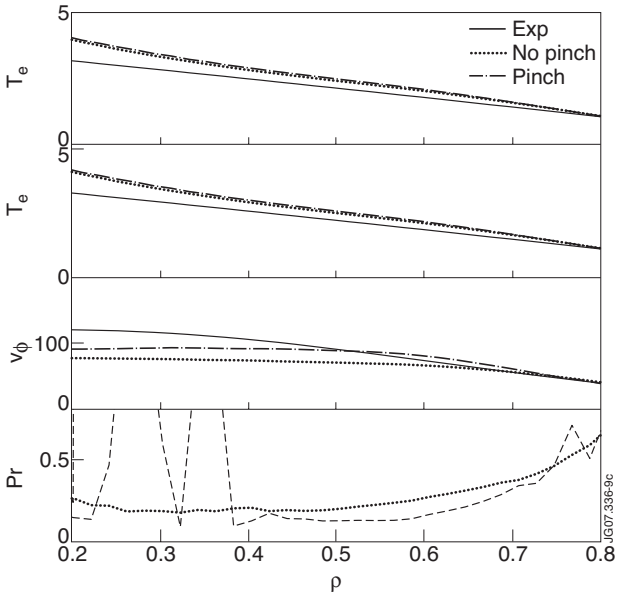

Figure 9: Experimental and predicted temperature and toroidal velocity profiles for JET Pulse No: 57894, with and without the momentum pinch in the simulations; predicted Prandtl numbers are also shown, with (dashed) and without (dotted) the pinch.